https://doi.org/10.5194/egusphere-2022-1502
Preprint. Discussion started: 23 January 2023

Modeling SOA contributions of VOC, IVOC and SVOC emissions and large uncertainties associated with OA aging

Ling Huang[1], Hanqing Liu[1], Greg Yarwood[2,*], Gary Wilson[2], Jun Tao[3], Zhiwei Han[4], Dongsheng Ji[5], Yangjun Wang[1], Li Li[1*]

[1]School of Environmental and Chemical Engineering, Shanghai University, Shanghai, 200444, China
[2]Ramboll, Novato, California, 94945, USA
[3]Institute for Environmental and Climate Research, Jinan University, Guangzhou, 510632, China
[4]University of Chinese Academy of Sciences, Beijing, 100049, China
[5]Institute of Atmospheric Physics, Chinese Academy of Sciences, Beijing, 100029, China

Correspondence to: Li Li (lily@shu.edu.cn), Greg Yarwood (gyarwood@ramboll.com)

Abstract

Secondary organic aerosols (SOA) are an important component of atmospheric fine particulate matter ($PM_{2.5}$) in China, and elsewhere, with contributions from anthropogenic and biogenic volatile organic compounds (AVOC and BVOC) and semi- (SVOC) and intermediate volatility organic compounds (IVOC). Policy makers need to know which SOA precursors are important but accurate simulation of SOA magnitude and contributions remains uncertain. We reviewed SOA modelling studies in the past decade that have reported the relative contributions of different precursors to SOA concentration and the findings have many inconsistencies due to differing emission inventory methodologies/assumptions, air quality model (AQM) algorithms, and other aspects of study methodologies. We investigated the role of different AQM SOA algorithms by applying two commonly used models, CAMx and CMAQ, with consistent emission inventories to simulate SOA concentrations and contributions for July and November 2018 in China. Both models have a volatility basis set (VBS) SOA algorithm but with different parameters and treatments of SOA photochemical aging. BSOA (SOA produced from BVOC) is found to be more important over southern China whereas SOA generated from anthropogenic precursors is more prevalent in the North China Plain (NCP), Yangtze River Delta (YRD), Sichuan Basin and Central China. Both models indicate negligible SOA formation from SVOC emissions as compared to other precursors. In July when BVOC emissions are abundant, SOA is predominantly contributed by BSOA (except for NCP), followed by IVOC-SOA (i.e. SOA produced from IVOC) and ASOA (i.e. SOA produced from anthropogenic VOC). In contrast in November, IVOC becomes the leading SOA contributor for all selected regions except PRD, illustrating the important contribution of IVOC emissions to SOA formation. Therefore, future control policies should aim at reducing IVOC emissions as well as traditional VOC emissions.

https://doi.org/10.5194/egusphere-2022-1502
Preprint. Discussion started: 23 January 2023

While both models generally agree in terms of the spatial distributions and seasonal variations of different SOA components, CMAQ tends to predict higher BSOA while CAMx generates higher ASOA concentrations. As a result, CMAQ results suggest that BSOA concentration is always higher than ASOA in November while CAMx emphasizes the importance of ASOA. Utilizing a conceptual model, we found that different treatment of SOA aging between the two models is a major cause of differences in simulated ASOA concentrations. The step-wise SOA aging scheme implemented in CAMx (based on gas-phase reactions with OH radical and similar to other models) exhibits a strong enhancement effect on simulated ASOA concentrations and this effect increases with the ambient OA concentrations. The CMAQ VBS implements a different SOA aging scheme that represents particle-phase oligomerization and has smaller impacts, or no impact, on total OA. A brief literature survey shows that different structure and/or parameters of the SOA aging schemes are being used in current models, which could greatly affect model simulations of OA in ways that are difficult to anticipate. Our results indicate that large uncertainties still exist in the simulation of SOA in current air quality models due to the aging schemes as well as uncertainties of the emission inventory. More sophisticated measurement data and/or chamber experiments are needed to better characterize SOA aging and constrain model parameterizations.

1 Introduction

Atmospheric fine particulate matter ($PM_{2.5}$) could reduce visibility (Kampa and Castanas, 2008), affect regional climate directly or indirectly (Liu et al., 2014), and exhibit adverse impacts on public health (Xie et al., 2014; Zhang et al., 2007). With the substantial emission reduction of sulfur dioxide (SO_2), nitrogen oxides (NO_x), and primary particles, the organic portion of $PM_{2.5}$ becomes increasingly important. Observations show that organic aerosols (OA) could contribute 30 – 70% of total $PM_{2.5}$ in China, with the secondary portion (i.e., secondary organic aerosols, SOA) accounting for a more significant portion than the primary portion (i.e., primary organic aerosols, POA) (Zhang et al., 2007). SOA is formed via chemical reactions of anthropogenic and natural precursors (e.g., volatile organic compounds, VOC) followed by subsequent gas-particle partitioning processes (Murphy et al., 2006). Due to gained polarity and hygroscopicity during aerosol aging, SOA is associated with stronger health impacts in cardiorespiratory mortality (Pye et al., 2021).

Meanwhile, numerical air quality models (AQM) are the tool used to evaluate the effectiveness of emission control policies, quantify regional contributions, and predict concentrations under future emission scenarios. However, accurate simulation of the magnitudes and variations of SOA via AQM has always been challenging due to the complexity of SOA itself and the complicated chemical processes involved in SOA formation. Numerous modelling studies have attempted to capture the temporal and spatial variations of observed SOA in China (Li et al., 2019; Li et al., 2020; Lin et al., 2016), with emphasis on

https://doi.org/10.5194/egusphere-2022-1502
Preprint. Discussion started: 23 January 2023

different aspects, including incorporating reactive surface uptake of dicarbonyls and isoprene epoxides (Chen et al., 2021; Liu et al., 2020), improve hydroxyl radical (OH) simulations by incorporating nitrous acid sources (Miao et al., 2021), and adding missing SOA precursors (Wu et al., 2021). The incorporation of semivolatile (SVOC, saturation vapor concentration (C^*) between 0.3 μg m^{-3} and 300 μg m^{-3} and intermediate volatility organic compounds (IVOC, C^* between 300 μg m^{-3} and 3 $\times 10^6$ μg m^{-3}; together referred to as S/IVOC) emissions as important SOA precursors has been a vigorously studied topic. Regional or national emission inventory of S/IVOC emissions were estimated based on either the conventional emission ratio method (i.e., ratio based on POA, VOC, or naphthalene) or using directly measured emission factor (Liu et al., 2017; Wu et al., 2021). Chang et al. (2022) proposed a full-volatility organic emission inventory recognizing that emissions of organic compounds have a continuous spectrum spanning from low to high volatility. Adding S/IVOC emissions or the full-volatility organic emissions in AQM has been shown to improve model simulated SOA concentrations, although uncertainties exist with the estimated S/IVOC emissions (Wu et al., 2021). For example, (Huang et al., 2021) applied the Comprehensive Air Quality Model with extensions (CAMx) to model SOA in the Yangtze River Delta (YRD) region, and IVOC emissions were shown to increase the simulated SOA concentration by 5%-26%. With an updated national S/IVOC emission inventory, the average deviation between simulated and observed SOA concentrations in China was reduced by 25% based on the WRF-Chem model (Wu et al., 2021).

Besides adding the SOA precursors, efforts have also been made to improve the modelling framework of SOA formation implemented in AQM (Donahue et al., 2009; Robinson et al., 2007). The two-product model and the volatility basis set (VBS) approach have been incorporated in commonly used AQM, with the former easy to implement while the latter better at capturing the SOA chemical aging (An et al., 2022; Lin et al., 2016; Yao et al., 2020). SOA simulation with the VBS scheme has been shown to generate more reasonable results than the two-product model (Huang et al., 2021; Lin et al., 2016). However, due to the complexity of the VBS scheme, quantifying SOA source contribution based on the VBS approach has been extremely limited and is mainly based on the brute-force method (An et al., 2022; Chang et al., 2022; Cheng et al., 2009), which is time-consuming and has limitations as a source apportionment method due to the nonlinearity of secondary pollutants like SOA. The Particulate matter Source Apportionment (PSAT; Yarwood et al., 2007) scheme implemented in CAMx (Ramboll 2020), built upon the two-product modelling scheme, can resolve SOA source attribution within a single model simulation while maintaining the overall model consistency. A more recent study by Dunker et al. (2019) combines the VBS scheme and the first-order sensitivity coefficients obtained by the decoupled direct method (DDM) to quantify source contributions to SOA in Houston, U.S., using the Path-Integral Method (PIM; Dunker,

https://doi.org/10.5194/egusphere-2022-1502
Preprint. Discussion started: 23 January 2023

2015).

Although substantial progress has been made in improving SOA simulation, inconsistent findings were reported among some recent SOA modelling studies in China, which warrants further investigation. For example, using the GEOS-Chem model, Miao et al. (2021) simulated much higher wintertime SOA concentrations over eastern China than summer-time SOA. In contrast, An et al. (2022) and Chang et al. (2022) reported slightly higher SOA in summer. Both Chang et al. (2022) and Wu et al. (2021) reported higher SOA formed from IVOC emissions (IVOC-SOA) than SVOC (SVOC-SOA), which is opposite to Miao's (2022) results showing much higher (by as much as two times) SVOC-SOA than IVOC-SOA in eastern China. The simulated SOA from conventional anthropogenic VOC (ASOA) also differs among studies. ASOA is estimated to be negligible (~0.25 μg m^{-3}) over the YRD region, and adding I/SVOC emissions increased SOA concentration by 116%, according to An et al. (2022). On the contrary, anthropogenic VOC (AVOC) are reported to contribute most to SOA formation (35.6 – 59.1%) and S/IVOC contributed the least (6.0 – 10.6%) in Li et al. (2022). These inconsistencies are potentially due to different S/IVOC emission inventories and different models being applied; thus, no clear conclusions can be drawn.

This study attempts to resolve some of the existing inconsistencies of simulated SOA based on two widely used air quality models in China, namely CAMx and CMAQ. These two models, with their abilities to track source attribution, have been frequently employed for air quality simulations in China. A publicly available national S/IVOC emission inventory developed for China was used to quantify the SOA contribution from different precursors. Similarities and differences in the simulated results from the two models are considered with a focus on contributions of different emission types (POA, VOC, IVOC, SVOC) and the SOA aging schemes which differ. Although both models are applied using a VBS scheme, the CAMx 1.5D VBS treats ASOA aging via gas-phase oxidation of the organic gases that exist in equilibrium with the SOA, whereas the CMAQ VBS treats ASOA aging via oligomerization of the condensed aerosol. Results from this study illustrate the uncertainties associated with SOA schemes in AQMs even when the model input data are harmonized. Revealing the important influence of SOA aging can stimulate future improvements to SOA modeling schemes.

2 Methodology

2.1 Model configuration

In this study, two commonly used air quality models - CAMx version 7.10 (Ramboll, 2021) and CMAQ version 5.3.2 (Appel et al., 2021) were used to simulate SOA concentrations in China for July (representing summer) and November (representing fall) of the calendar year

https://doi.org/10.5194/egusphere-2022-1502
Preprint. Discussion started: 23 January 2023

2018. The models are applied over the same domain with input data developed from the same sources, although each model has its own processes for handling input data. The modeling domain covers the entire China with a spatial resolution of 36 km (Figure 1). The Weather Research and Forecasting (WRF) model (version 4.0, (Skamarock and Klemp, 2008) was applied to simulate meteorological fields, and WRF model configurations were summarized in our previous studies (Huang et al., 2021). Anthropogenic emissions within China utilized the Multi-resolution Emission Inventory for 2017 (MEIC, http://www.meicmodel.org, accessed on 25th September 2021) developed by Tsinghua University; emissions outside China are based on the Emissions Database for Global Atmospheric Research (EDGAR, http://edgar.jrc.ec.europa.eu/index.php, accessed on 25th September 2021) for the year 2010. Specifically, MEIC provides VOC emissions speciated for Carbon Bond 2005 (CB05) and SAPRC 2007 (SAPRC07), which were combined to generate speciated VOC emissions for the CB6 mechanism (see details in Supporting Information). Biogenic emissions were calculated using a recent offline version of the Model of Emissions of Gases and Aerosols from Nature (MEGAN version 3.2, http://aqrp.ceer.utexas.edu/projects.cfm, accessed on 25th September 2021).

The CAMx model configuration included the CB6 photochemical gas-phase mechanism (Yarwood et al., 2010), the static two-mode coarse/fine (CF) PM chemistry option with ISORROPIA inorganic gas-aerosol partitioning scheme (Nenes et al., 1998), the Regional Acid Deposition Model (RADM) aqueous phase chemistry, the Zhang dry deposition option (Zhang et al., 2003) and wet deposition. In terms of the SOA modeling scheme, CAMx provides the option to select one of two schemes: a traditional two-product scheme (named SOAP) or a 1.5-D VBS scheme which is a simplified version of the 2-D VBS scheme (Koo et al., 2014). This study used the CAMx 1.5D VBS scheme because it is more similar than SOAP to the CMAQ VBS SOA scheme. Compared with the SOAP scheme, the 1.5-D VBS scheme treats POA as being semivolatile and includes multi-stage aging of SOA with both oxidation and fragmentation occurring to describe the evolution of OA in terms of oxidation state and volatility. For CMAQ simulations, the model configuration included the CB6 gas-phase mechanism, the AERO7 aerosol scheme (Appel et al., 2021), the RADM aqueous phase chemistry, and ISORROPIA inorganic particulate thermodynamics. Both CMAQ and CAMx consider SOA formation from traditional anthropogenic VOC (e.g., benzene, toluene, and xylene) and biogenic VOC (i.e., isoprene and monoterpenes), but there are several differences. For example, CMAQ includes SOA formation from isoprene oxidation production (IEPOX) in the aqueous phase. An important difference between the CAMx and CMAQ VBS schemes is that in CAMx, each volatility bin can be oxidized continuously to the next lower volatility bin in a step-wise manner providing a dynamic SOA volatility distribution, whereas in CMAQ the SOA is not oxidized and so maintains a static volatility

https://doi.org/10.5194/egusphere-2022-1502
Preprint. Discussion started: 23 January 2023

distribution. This point will be discussed more in Section 3.4.

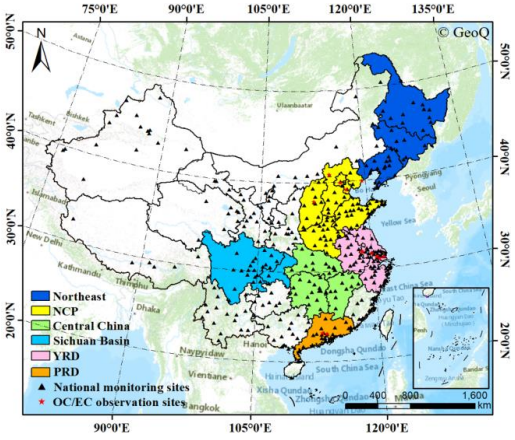

Figure 1 Modeling domain in this study with definitions of key regions and locations of national monitoring sites (in black triangles) in 364 major cities and sites with OC/EC observations (in red star) in 13 cities.

2.2 S/IVOC emissions

To evaluate the contributions of S/IVOC emissions to SOA formation, we included a gridded (0.25 °×0.25 °) monthly S/IVOC emission inventory from industry, residential, transportation, power plants, and shipping for the year 2016 (Wu et al., 2019). The total reported SVOC and IVOC emissions were 2,881 and 6,718 Gg, respectively, with industry and residential sectors being the dominant contributor. For SVOC emissions on an annual scale, industrial and residential sources accounted for 12.6% and 64.6%, respectively; for IVOC emissions, these two sectors accounted for 63.1% and 15.5%, respectively. Spatially, S/IVOC emissions are mainly distributed in China's highly industrialized and urbanized regions, for example, the Beijing-Tianjin-Hebei (BTH) and YRD regions (Wu et al., 2021). Regarding the monthly variations, S/IVOC emissions are higher in winter (due to residential sources) and lower in summer, with winter season (i.e., three months) emissions accounting for 31% of annual total emissions.

For the CAMx simulations, IVOC were labelled as 'IVOG', 'IVOD', 'IVOB', and 'IVOA', each representing IVOC emissions from gasoline engines, diesel engines, biomass burning, and other anthropogenic sources; the corresponding SVOC was renamed as 'POA_GV', 'POA_DV', 'POA_BB' and 'POA_OP' (Ramboll, 2021). In CMAQ simulations, IVOC were renamed pcVOC (Murphy et al., 2017), and SVOC were allocated into POC and PNCOM based on existing ratios provided in CMAQ (see Table S2 for details).

https://doi.org/10.5194/egusphere-2022-1502
Preprint. Discussion started: 23 January 2023

2.3 Simulation scenarios

In order to evaluate the impact of different models and S/IVOC emissions on simulated SOA concentration, three sets of parallel simulations (each set with CMAQ and CAMx, respectively, so a total of six) were conducted for July and November 2018 with identical meteorological fields (Table 1). In the base scenario, only the conventional anthropogenic emissions and biogenic emissions were included. In the other two scenarios, IVOC emissions or S/IVOC emissions were included, respectively. The contribution of IVOC and SVOC emissions to SOA was quantified by subtracting base case results (e.g., CAMx_IVOC minus CAMx_base to get IVOC contribution, etc.). Different OA components, including POA, anthropogenic SOA (ASOA), and biogenic SOA (BSOA), were distinguished in each scenario because they are resolved by the model OA schemes.

Table 1 Model scenarios

Scenario	AQM	Anthropogenic VOC emissions	IVOC emissions	SVOC emissions
CAMx_base	CAMx v7.10	MEIC	none	none
CAMx_IVOC		MEIC	Wu et al. (2021)	none
CAMx_S/IVOC		MEIC	Wu et al. (2021)	Wu et al. (2021)
CMAQ_base	CMAQ v5.3.2	MEIC	none	none
CMAQ_IVOC		MEIC	Wu et al. (2021)	none
CMAQ_S/IVOC		MEIC	Wu et al. (2021)	Wu et al. (2021)

2.4 $PM_{2.5}$ and OC/EC observations

Simulated concentrations of $PM_{2.5}$ and SOA were compared against surface observations of hourly $PM_{2.5}$ at 364 national monitoring sites and organic carbon (OC)/elemental carbon (EC) were compared at a limited number of sites. Observations of $PM_{2.5}$ were obtained from the China National Environmental Monitoring Centre (http://www.cnemc.cn/, accessed on 25th September 2021). Hourly observed OC/EC during July and November 2018 at 13 monitoring sites (see detailed locations and observation periods in Table S3) were used to evaluate simulated SOA by applying the minimum OC/EC ratio method (Cao et al., 2004; Castro et al., 1999) to the observations. The OC/EC sites were mainly located in North China, East China, and South China. An OA/OC ratio of 1.6 is used to convert SOC/OC to SOA/OA for direct model comparison (Feng et al., 2009). Model performance was evaluated based on commonly used statistical metrics, including the mean bias (MB), normalized mean bias (NMB), normalized mean error (NME), and FAC2 (see Table S4 for definitions).

https://doi.org/10.5194/egusphere-2022-1502
Preprint. Discussion started: 23 January 2023

3 Results and discussions

3.1 Brief review of existing SOA simulation studies in China

Table 2 summarizes existing SOA simulation studies conducted using different AQMs in China during the past ten years. Earlier studies used two-product SOA schemes and generally underestimated SOA. For example, based on the two-product scheme implemented in WRF-Chem, Jiang et al. (2012) found a maximum underestimation of 75% in simulated SOA during 2016 over China. In another study by Li et al. (2017), although simulated SOA concentration increased nearly four times after increasing aromatic emissions and changing SOA yields, the model still underestimated observed SOA by 72% on average. To better represent the physical and chemical attributes of SOA in AQMs, Donahue et al. (2006) introduced the VBS scheme, which considers gas-aerosol partitioning and chemical aging of both POA and SOA. Compared to the two-product approach, VBS is shown to improve model simulations of SOA substantially. Han et al. (2016) simulated SOA in eastern China and found that the VBS approach could well reproduce the observed SOA at four monitoring sites both in magnitudes (2.8 $\mu gC/m^3$ vs. observed value of 3.3 $\mu gC/m^3$) and in terms of the SOA/OA ratio (33% vs. observed value of 32%). Lin et al. (2016) applied the VBS approach in CAMx to simulate SOA concentration and source attribution in Beijing urban area in the summer; results show that the VBS approach substantially improved simulated SOA concentration (from 0.73 $\mu g/m^3$ to 5.3 $\mu g/m^3$ at a station in Beijing); however, the model still under-predicted observed SOA values with NMB of -72%. Besides improving the SOA modeling scheme, the inclusion of S/IVOC emissions (in addition to VOC) as missing SOA precursors was also reported with improved performance of SOA simulations. Based on a national S/IVOC emission inventory developed for six sectors (i.e., industry, residential, transportation, power plants, shipping, and biomass burning), simulated SOA concentration increased by 122% in the PRD region and the fraction of observed SOA resolved by model increased from 18% to 40%. In YRD, Huang et al. (2021) found that the simulated SOA concentration could increase by up to 75.6% with the addition of IVOC emissions under the VBS scheme, but simulated OA was 38.5% lower than observations. In a most recent study by Chang et al. (2022), a full-volatility organic emission inventory developed for China was shown to better reproduce observed OA concentrations as well as the split between POA and SOA. Other efforts to improve SOA simulation include adding SOA formation from reactive surface uptake of dicarbonyls and IEPOX/MAE (Hu et al., 2017), updating SOA yields from S/IVOC, considering additional nitrous acid sources to enhance precursor oxidation rates (Miao et al., 2021), incorporation of O_3^- and NO_3^- initiated SOA formation pathways (Wu et al., 2021).

https://doi.org/10.5194/egusphere-2022-1502
Preprint. Discussion started: 23 January 2023

As shown by Table S5, various S/IVOC emission inventories have been developed for different sources and regions, yet large uncertainties exist. For example, Liu et al. (2017) obtained a national total of 200.4 Gg IVOC from mobile sources for the year 2015 based on the emission factor method, which is slightly lower than the value (241.2 Gg) reported by Wang et al. (2022) and much higher than Wu's result (134.4 Gg; Wu et al. 2019) based on the IVOC/POA ratio. Using three different estimation methods, Miao et al. (2017) reported a range of 3.8 – 6.6 Tg anthropogenic IVOC emissions for 2014 in China, which is 30% – 60% lower than the value (9.6 Tg) reported by Wu et al. (2021) for 2016. Regionally, Huang et al. (2021) calculated the IVOC emissions in the YRD region, and IVOC emissions could be different by a factor of 6.4 – 69.5 when different methods were applied. The relative contributions from different sources also differ among studies, further increasing the uncertainties of SOA source tracking. Chang et al. (2022) indicate that domestic combustion (including fossil fuel and biomass) and open biomass burning represents the dominant contributors to S/IVOC emissions. In contrast, industry and residential sources contribute 78% of total S/IVOC emissions, according to Wu et al. (2021). These results indicate significant uncertainties associated with S/IVOC emission inventory and warrant more measurement data to better constrain the emission estimation in the future. In this study, we utilized the emission inventory developed by Wu et al. (2021) and focused on the similarities and differences between the models while temporarily ignoring the uncertainties associated with the S/IVOC emission inventory itself.

https://doi.org/10.5194/egusphere-2022-1502
Preprint. Discussion started: 23 January 2023

Table 2 Summary of findings from SOA simulation studies in China

Reference	Model	Year/Season	Region	SOA modeling scheme	S/IVOC emissions	Summary of findings
Fu et al. 2011	GEOS-Chem	2006/all four seasons	China	two-product	No	Secondary formation accounts for 21 % of Chinese annual mean surface OC in the model
Jiang et al. 2012	WRF-Chem	2006/all four seasons	China	two-product	No	The model well captured spatial and temporal characteristics of OC and EC, but the simulated SOA concentration was underestimated by up to 75%.
Li et al. 2017a	RAMS-CMAQ	2014/fall	China	two-product	No	By increasing aromatic emissions and modifying model parameters, simulated SOA concentration increased by nearly four but still underestimated the observed SOA by an average of 72%.
Lin et al. 2016	WRF-CAMx	2007/summer	BTH	VBS	No	VBS approach substantially improved hourly, daily, and monthly SOA simulations but still largely underestimated observed SOA with a normalized mean bias of -72%.
Han et al. 2016	RAQMS[a]	2009/spring	East China	VBS	No	Adopting the VBS approach with chemical aging suggests ASOA is the dominant SOA component over east China in springtime.
Zhao et al. 2016a	WRF-CMAQ	2010/all four seasons	China	VBS	Yes	OA aging and IVOC emissions increase OA and SOA concentrations in China by about 40%.
Li et al. 2016	RAMS-CMAQ	2014/winter	China	VBS	No	Updated to incorporate SOA production from isoprene and sesquiterpenes and to account for the SOA production rate dependence on NOx and SOA aging. Modeled monthly mean SOA concentrations were high in central and eastern China and low in western regions.
Hu et al. 2017	WRF-CMAQ	2013/all four seasons	China	VBS	No	The model included the treatment of isoprene gas-phase chemistry that leads to the production of IEPOX and MAE. It also includes an updated SOA mechanism with updated VBS and SOA formation from reactive surface uptake of dicarbonyls, IEPOX, and MAE.
Wu et al. 2019	WRF-Chem	2008/winter	PRD	VBS	Yes	The simulated SOA increased by 161% with the input of S/IVOC emissions over the PRD region.
Li et al. 2020	WRF-NAQPMS	2014/winter	China	VBS	Yes	After adding S/IVOC emissions, the maximum concentration of SOA reached up to 50 μg/m^3 in Beijing and Shijiazhuang. SOA/OA ratio is around 50% in most areas of the BTH region.
Liu et al. 2020	WRF-CMAQ	2015/winter 2016/winter	YRD	VBS	No	Based on the updated SAPRC-11 mechanism, observed and predicted SOA concentrations were 6.4 μg m^{-3} and 6.9 μg m^{-3} in the winter of 2015 and 5.7 μg m^{-3} and 9.6 μg m^{-3} in the winter of 2016.
Li et al.2020	CMAQ	2013/winter, summer	Eastern China	two-product	No	The impact of water vapor partitioning and nonideality of the organic-water mixture on SOA formation is considered in the model. The modified model well captured observed diurnal OA variations in winter but didn't capture peak values under polluted days with a mean fractional bias of -20%.
Wu et al. 2021	WRF-Chem	2017/winter	China	VBS	Yes	With the addition of S/IVOC emissions, the fraction of observed SOA resolved by the model increased from 18% to 40%.
Huang et al. 2021	WRF-CAMx	2018/summer	YRD	VBS/two-product	Yes	With 1.5 D-VBS and IVOC emissions, simulated SOA concentration increased by 61% in the YRD region, and SOA/OA ratio matched well with observed values.
Miao et al. 2021	GEOS-Chem	2014/summer, winter	China	VBS	Yes	With updated emissions, volatility distributions, and SOA yields of SVOC and IVOC and the addition of HONO sources, anthropogenic SVOC and IVOC are shown to be the dominant source of SOA, with a contribution of over 50% over most of China.
An et al. 2022	WRF-CMAQ	2019/spring, summer 2018/autumn, winter	YRD	VBS	Yes	After adding the S/IVOC emissions inventory, the simulated SOA values in the YRD region increased by 116%. Industry is found to contribute the most to SOA concentration in YRD.
Chang et al. 2022	CMAQ	2017/winter, summer	China	2D-VBS	Yes	A full-volatility organic emission inventory was developed and was shown to better reproduce observed OA concentration and SOA/OA ratio. Volatile chemical products (VCPs), domestic combustion, and biomass open burning are three leading sources of SOA.
Li et al. 2022	WRF-RAQMS	2018/summer	Eastern China	VBS	Yes	After adding to the S/IVOC emissions inventory, SOA formation from S/IVOC emissions was lower in summer than in winter. Enhanced contribution to SOA from aqueous uptake and reaction of GLY and MGLY in summer than in winter were modeled.

https://doi.org/10.5194/egusphere-2022-1502
Preprint. Discussion started: 23 January 2023

3.2 Model performance evaluation

Figure 2 shows the spatial distribution of monthly averaged $PM_{2.5}$ concentration simulated under CAMx_S/IVOC and CMAQ_S/IVOC scenarios. Overall, the two models are able to capture the spatial distributions and seasonal variations of observed $PM_{2.5}$ with MB of -4.1 – 8.3 μg m^{-3}, NMB of -17.1 – 17.5%, and NME of 37 – 49%. Values of NMB and NME meet the criteria standards (NMB within 20% and NME within 45%, except for CAMx NME) proposed by Huang et al. (2021), indicating acceptable model performance for $PM_{2.5}$. Regionally, simulations over NCP and Sichuan Basin show an overestimation with MB of -8.2 – 24.8 μg m^{-3} and NMB of -16.0 – 59.6% (Table S6). CAMx generally tends to simulate higher $PM_{2.5}$ concentrations (by 13.4 – 60.2%) than CMAQ. We further evaluated simulated SOA at a limited number of observation sites (Figure S1 and Figure S2), noting that the "measured" SOA is diagnosed from measurements of total OC as discussed above. Model performance for simulated SOA varies across different sites, with a general pattern of overestimation in July and underestimation in November (Table S7).

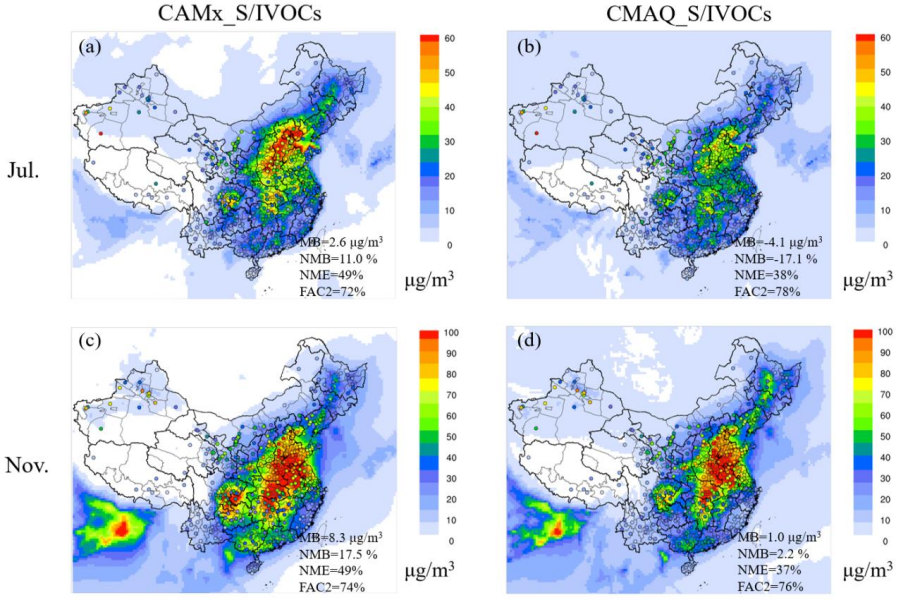

Figure 2 Spatial distributions of simulated and observed (filled circles) $PM_{2.5}$ concentration (μg/m) in July (upper row) and November (bottom row) 2018 based on CAMx (left column) and CMAQ (right column) simulations including S/IVOC emissions.

3.3 OA components simulated by CAMx and CMAQ

Figure 3 shows the spatial distribution of different OA components simulated by CAMx and CMAQ for July and November. Five OA components, including POA, ASOA, IVOC-SOA, SVOC-SOA, and BSOA, were identified either as direct model outputs (POA, and BSOA) or

https://doi.org/10.5194/egusphere-2022-1502
Preprint. Discussion started: 23 January 2023

obtained as the differences between different modeling scenarios listed in Table 1. Table S8 shows the domain averaged concentration for each OA component by selected regions.

Primary organic aerosols (POA)

POA represents organic aerosols that are directly emitted from anthropogenic sources (e.g., residential wood combustion). In the VBS scheme, POA is allowed to vaporize into gaseous phase and undergo further oxidation processes to form SOA. The magnitudes and spatial distributions of POA agree well between CAMx and CMAQ results as well as previous studies (e.g., Hu et al., 2017), with high concentrations simulated over Northeast China, NCP, northern YRD, and Sichuan Basin. Seasonally, simulated POA concentration in November is much higher than July as a result of higher emissions. In July, POA ranged from 0.3 μg m^{-3} (CMAQ PRD) to ~1.9 μg/m^3 (CAMx Sichuan Basin) and accounts for less than 10% of the total OA concentrations for all selected regions, except Sichuan Basin (~15%), suggesting a relatively minor role compared to SOA during the summer season. In November, domain-averaged POA ranged from 1.3 μg/m^3 (CMAQ PRD) to ~ 6.7 μg/m^3 (CMAQ Northeast) and became the dominant OA component in Northeast China (~70%). For other regions in November, POA contributed from ~10% (in PRD) to ~40% (in NCP) of the total OA concentration, suggesting that SOA is still the dominant OA component for most regions.

Secondary organic aerosols (SOA)

Except for Northeast China in November, SOA concentration exceeds that of POA and different SOA components show distinctly different seasonal and spatial variations. Biogenic SOA (BSOA) is mainly concentrated over the southern part of China where BVOC emissions are abundant, whereas anthropogenic-oriented SOA (i.e., ASOA and IVOC-SOA) are mainly concentrated over the northern part of China in July and shifted southward in November. Seasonally, BSOA concentration is much higher in July, with maximum monthly-averaged BSOA concentration exceeding 15 μg/m^3 over specific areas in Central China. In contrast, ASOA and IVOC-SOA concentrations are higher in November for most of the regions. Figure 4 and 5 shows the subdomain averaged relative contribution of different OA components for selected regions. In July, BSOA represented the dominant SOA component (except NCP), accounting for 45.5% – 60.2% in the Northeast to as much as 71.5% – 82.7% in Central China. In November when BVOC emissions are dramatically lower, the relative contribution of BSOA decreases sharply. Nevertheless, BSOA still represents the most abundant SOA component (by 37.1% – 51.0%) for PRD in November. The two models simulate similar IVOC-SOA concentrations with a maximum of up to 7.3 μg/m^3 in July and 8.7 μg/m^3 in November. The relative contribution of IVOC emissions to SOA ranged from 13.4% – 13.8% in PRD to 35.0% – 42.5% in NCP for July and 26.3% – 29.7% in PRD to 51.4% – 62.5% in

https://doi.org/10.5194/egusphere-2022-1502
Preprint. Discussion started: 23 January 2023

NCP for November, suggesting an important contribution of IVOC emissions to SOA, especially during November. Compared to other components, both models suggest that SOA generated from SVOC emissions (i.e., SVOC-SOA) are negligible (<0.5 μg m^{-3}), accounting for less than 5% of SOA concentration for most regions.

Differences are observed in the magnitude of simulated BSOA and ASOA concentrations between the two models, although the spatial distributions and seasonal variations are consistent. On the one hand, CMAQ tends to simulate slightly higher BSOA concentrations than CAMx. For example, the domain averaged BSOA concentration over NCP in July is 2.8 μg/m^3 based on CAMx results, which is 22.2% lower than that of CMAQ. For Central China where BVOC emissions are abundant, BSOA estimated from CAMx in July (10.8 μg/m^3) is 33.1% lower than CMAQ (14.8 μg/m^3). In November, the relative differences in BSOA between the two models become even larger, although the absolute magnitudes are lower compared to July. The higher BSOA simulated by CMAQ is likely associated with recent modifications implemented in CMAQ: (1) the yield of organic aerosol from monoterpene oxidation was increased; and (2) alpha-pinene was treated explicitly in the model and 30% of the total terpenes emissions were allocated to alpha-pinene (US EPA, 2019). However, we did not investigate this difference because our study focuses on anthropogenic emissions. On the other hand, CAMx predicts much higher ASOA concentration than CMAQ, by up to ~4 times higher in July and ~2 times higher in November. For instance, CAMx simulated ASOA concentration in NCP is 5.7 μg/m^3 for July as opposed to 1.4 μg/m^3 by CMAQ. In November, CAMx simulated ASOA concentration in YRD is 4.1 μg/m^3 compared to 2.4 μg/m^3 by CMAQ. This difference in simulated ASOA concentration is discussed in detail in Section 3.4. Because of these differences, the relative contribution of ASOA and BSOA varies between the two models. For CAMx simulations, ASOA accounts for 10.9% (Central China) – 42.1% (NCP) of total SOA concentration in July and 23.6% (Northeast China) – 38.7% (Sichuan Basin) in November. For CMAQ simulation, the relative SOA contribution of ASOA ranges from 4.3% (Central China) – 15.0% (NCP) in July and 16.3% (PRD) – 21.8% (YRD) in November. In November, CMAQ results suggest that BSOA concentration is always higher than ASOA, while CAMx emphasizes the importance of ASOA more than BSOA.

https://doi.org/10.5194/egusphere-2022-1502
Preprint. Discussion started: 23 January 2023

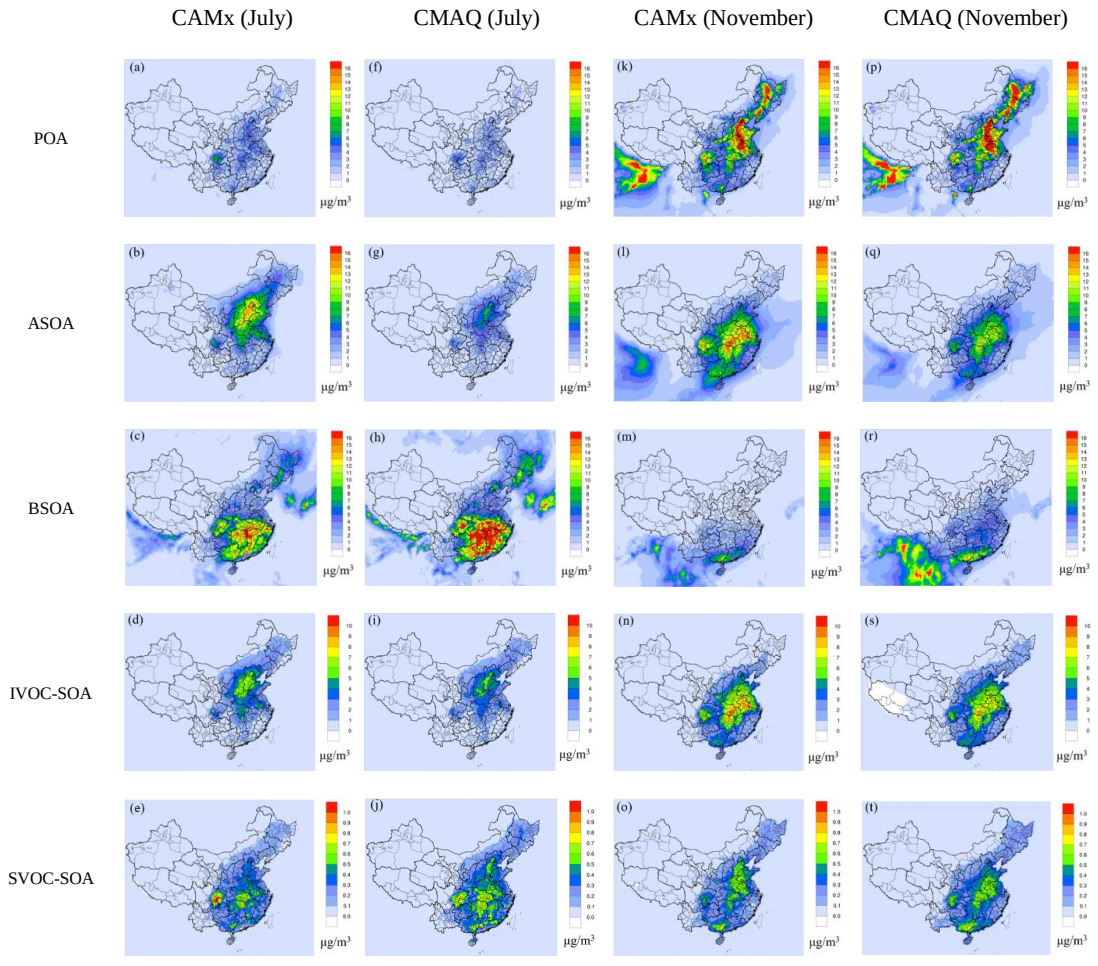

Figure 3 Spatial distributions of different OA components in July and November

https://doi.org/10.5194/egusphere-2022-1502
Preprint. Discussion started: 23 January 2023

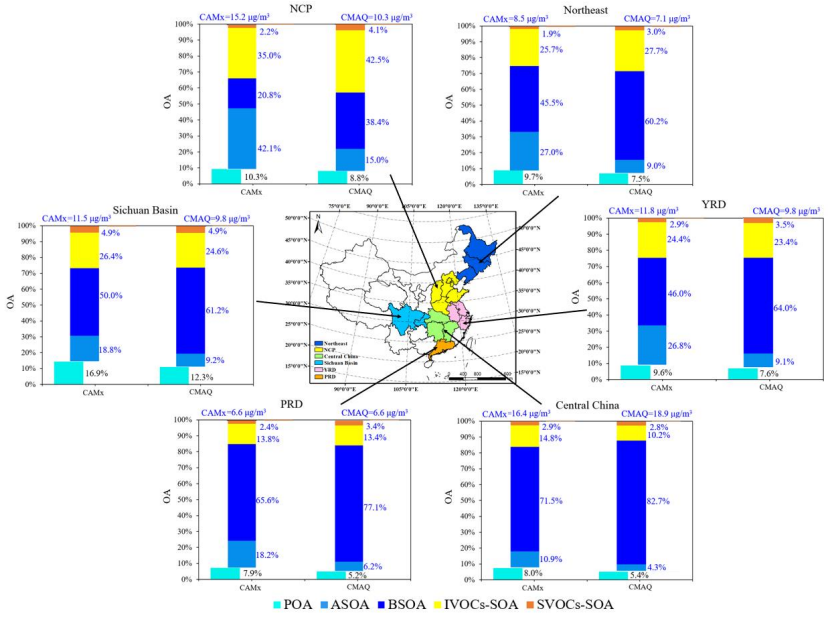

Figure 4 Domain-averaged OA concentration (labelled on top) and relative contributions of different components (labelled inside Figures) in July 2018 (Note that the relative contributions of ASOA, BSOA, IVOC-SOA, and SVOC-SOA sum to 100%).

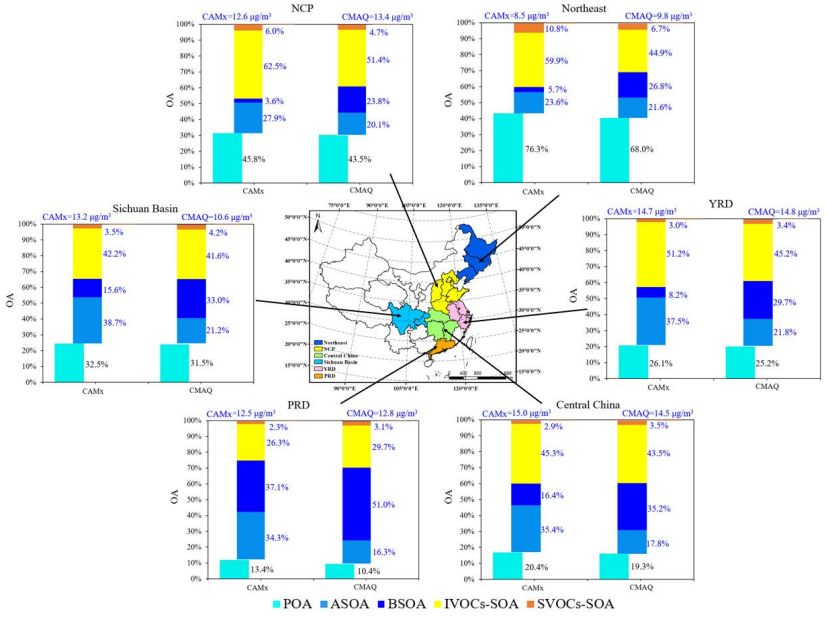

Figure 5 Domain-averaged OA concentration (labelled on top) and relative contribution of different components (labelled inside Figures) in November 2018 (Note that the relative contribution of ASOA, BSOA, IVOC-SOA, and SVOC-SOA sum to 100%).

https://doi.org/10.5194/egusphere-2022-1502
Preprint. Discussion started: 23 January 2023

3.4 Accounting for SOA aging

Although a VBS scheme is implemented in both CAMx and CMAQ, substantial differences were found in the simulated ASOA concentrations, as shown above, with CAMx predicting much higher values than CMAQ (Figure 4 and Figure 5). For example, simulated domain-averaged ASOA concentration in July by CAMx is 5.7 μg/m^3 and 2.9 μg/m^3 over NCP and YRD, respectively, but the corresponding values simulated by CMAQ are only 1.4 μg/m^3 and 0.8 μg/m^3, which are approximately four times lower. The relatively high ASOA concentrations from CAMx results are consistent with the study by Li et al. (2022), who applied the regional air quality model system (RAQMS) over east China and reported 48.3% of SOA was formed from AVOC emissions. Meanwhile, the much lower ASOA concentrations simulated by CMAQ in July over the YRD region (domain-average: 0.8 μg/m^3) are consistent with another CMAQ study conducted by An et al. (2022), who showed minimal SOA contribution (<0.5 μg/m^3) from AVOC for all four seasons. The significant differences in simulated ASOA concentrations between the two models are explained by two aspects of the VBS implementation. First, the SOA molar yields from anthropogenic VOC (i.e., benzene, toluene, and xylene) are different in the two models, especially under low-NO*x* conditions (Table S9). For instance, under the low-NO*x* conditions, CMAQ SOA is only formed in the least volatile bin (C^*=0.01 μg/m^3), whereas CAMx SOA is formed in different bins with volatility ranging from 1 μg/m^3 to 100μg/m^3. The total VBS yield (summed over VBS bins) also differs between the models, as exemplified by the total yield for benzene being 0.146 in CMAQ vs. 0.596 in CAMx for low-NO_x conditions (Table S9). The total VBS yield does not translate directly into SOA yield because the effects of bin volatility (C*) and aging must also be considered, as illustrated below. Nevertheless, the total VBS yields for anthropogenic VOC are higher in CAMx than CMAQ for all precursors and high/low NO_x conditions. This difference can be explained, in part, by the influence of wall-losses on chamber experiments that are used to characterize SOA formation and derive VBS product distributions. The CAMx 1.5D VBS SOA yields are corrected for vapor wall losses in smog chamber experiments (Hodzic et al., 2016; Zhang et al., 2014) whereas the CMAQ VBS SOA yields are not wall-loss corrected (personal communication from Dr. Havala Pye, U.S. EPA).

The second major difference between the two models lies in the treatment of SOA aging. In the CAMx 1.5D VBS, gas-phase oxidation products in different volatility bins are continuously oxidized by reactions with OH (with an OH rate constant of 2×10^{-11} cm^3/molecule/s) that move mass from higher volatility bins to the next lower volatility bin in a step-wise manner (for example, from C^*=1000 μg/m^3 to C^*=100 μg/m^3 and from C^*=100 μg/m^3 to C^*=10 μg/m^3). The CAMx aging scheme will tend to produce more extensive aging in summer than winter due to higher OH concentrations and greater evaporation of SOA to

https://doi.org/10.5194/egusphere-2022-1502
Preprint. Discussion started: 23 January 2023

the gas-phase in warmer conditions. In contrast, the CMAQ VBS has no gas-phase oxidation of VBS products and instead converts SOA in VBS bins with C^*= 1 μg/m^3 to C^*=100 μg/m^3 directly to non-volatile SOA at a constant rate of 3.4% per hour. The CMAQ aging scheme, representing oligomerization, will tend to produce more extensive aging in winter than summer due to greater condensation of SOA in colder conditions.

We investigated how the different treatments of SOA aging in the CMAQ and CAMx VBS schemes influence simulated SOA concentrations by performing simple conceptual calculations outside the models. Based on Pankow's partitioning theory (Pankow, 1994), the SOA yield α from a specific precursor (e.g., benzene) is calculated using Eq. (1):

$$\alpha = \sum_{i}^{N} \beta_i \left(1 + \frac{C_i^*}{C_{OA}}\right)^{-1} \quad \text{Eq. (1)}$$

where β_i is the mass yields from each volatility bin (i), which are the values listed in Table S9; C_i^* is the volatility defined for each bin, and C_{OA} is the total ambient OA concentration. We first consider a scenario with no aging in CAMx (CAMx_no-aging). Taking benzene as an example and assuming C_{OA} = 1 μg/m^3 in Eq. (1), SOA mass yield (dimensionless units) from benzene under high and low-NO*x* conditions is 0.009 and 0.029, respectively. With ambient C_{OA} increased by ten times (i.e., C_{OA} = 10 μg/m^3), the gas-particle partition equilibrium shifts more towards the particle phase and the SOA mass yield for benzene increases to 0.056 and 0.105 for high and low-NO*x*, respectively. Thus we obtain the SOA mass yields for benzene as a function of C_{OA} shown by solid lines in Figure 6 (similar calculations for toluene and xylene are presented in Figure S3). Similarly, for CMAQ with no aging (CMAQ_no-aging) and C_{OA} = 1 μg/m^3, the SOA mass yield from benzene is 0.021 and 0.145 under high-and low-NO*x* conditions, respectively. As C_{OA} increased to 10 μg/m^3, SOA mass yield remained unchanged under low-NO*x* conditions and increased by a factor of 3.2 under high-NO*x* conditions, as shown by dashed lines in Figure 6. When oligomerization (aging) over 6 hours is considered in CMAQ (CMAQ_aging), SOA yield for benzene is enhanced by approximately a factor of 2 under the high-NO*x* condition, but there is no enhancement under low-NO*x* condition because the CMAQ VBS always treats this aerosol as being non-volatile and therefore unaffected by aging.

The effect of aging can be much stronger in CAMx than in CMAQ, depending upon the modeled OH radical concentration. We performed a simple offline sensitivity analysis assuming a representative winter OH concentration of 5×10^5 molecules/cm^3. As shown in Figure 7, an initial VBS distribution favoring higher volatility bins (i.e., towards bin 5) evolves over time with aging (i.e., OH-reaction of the gas-phase fraction in each bin) to favor lower volatility bins (i.e., towards bin 1) which reduces overall volatility and increases aerosol

https://doi.org/10.5194/egusphere-2022-1502
Preprint. Discussion started: 23 January 2023

yield. An OH exposure of 10^{10} molecules/cm^3, equal to an exposure time of 5.75 hr, was used so that the aging effects shown for CAMx and CMAQ are for a similar duration. With this amount of aging/oxidation effect, the VBS bin molar yields for benzene under high-NO*x* become 0.130, 0.580, 0.400, 0.177, and 0.048 as compared to 0.035, 0.108, 0.185, and 0.268 with no aging (see Table 6). These aged yields are converted to SOA mass yields under different total OA concentrations using Eq. (1), as shown by the red symbol line in Figure 8. For a C_{OA} = 1 μg/m^3 with ~6 hours of aging, CAMx simulated a SOA mass yield of 0.322 from benzene under the high-NO*x* condition as opposed to 0.009 without aging, an enhancement greater than a factor of 30. This aging effect becomes even stronger as the ambient OA concentration increases. These conceptual calculations reveal significant differences in the magnitude of SOA enhancement produced by SOA aging applied with the CAMx and CMAQ VBS schemes.

A literature review reveals that different treatments of SOA aging, or no aging, are widespread in the application of VBS schemes. For example, Hayes et al. (2015) applied box models with multi-generating aging parameterization to simulate SOA in Los Angeles during CalNex 2010, which was shown to over-predict urban SOA at photochemical age larger than 1 day. With several alternate model configurations, Dzepina et al. (2011) predicted SOA mass in Mexico City during MILAGRO 2006 and found that a scenario with multi-generational SOA aging scheme and no S/IVOC emissions could successfully predict observed SOA but adding S/IVOC emissions resulted in large over-predictions. Jiang et al. (2012) applied WRF-Chem to simulate SOA in China with no aging scheme and concluded that omitting chemical aging of SOA and POA might be the main reason for their underestimation of SOA by up to 75%. Han et al. (2016) contrasted simulated SOA results based on the VBS scheme with and without considering aging in RAQMS and found that a VBS scheme with aging under-estimated SOA by only 15%, whereas VBS without aging under-estimated SOA by 70%.

The examples of differing OA model assumptions and outcomes found in this brief literature review and in our simulation results emphasize that model simulations of OA are very sensitive to whether and how SOA aging is represented. A diverse variety of VBS schemes are being used in air quality models and the predicted OA concentrations may depend upon scheme structure and/or parameters in ways that are difficult to anticipate. Comparing SOA yield curves under idealized conditions (e.g., Figure 6) can be helpful for comparing different schemes. The range of outcomes produced by current OA schemes illustrates that large uncertainties remain, as well as uncertainties in emission inventories that should be considered when interpreting results from OA modeling studies. There is a continuing need for sophisticated measurement data to provide better constraints.

https://doi.org/10.5194/egusphere-2022-1502
Preprint. Discussion started: 23 January 2023

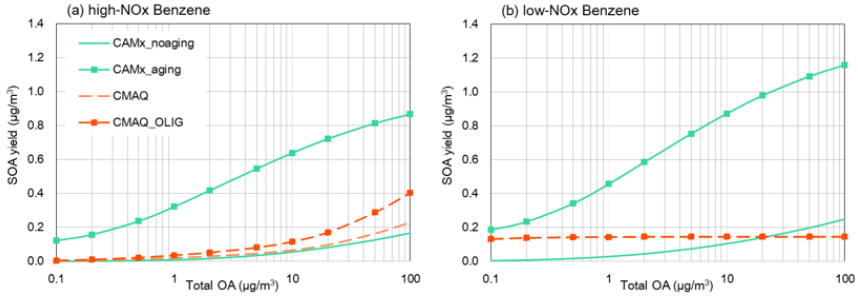

Figure 6 Conceptual SOA mass yield (μg/m^3 SOA formed per μg/m^3 precursor reacted) from benzene under (a) high- and (b) low-NO*x* conditions by different model configurations

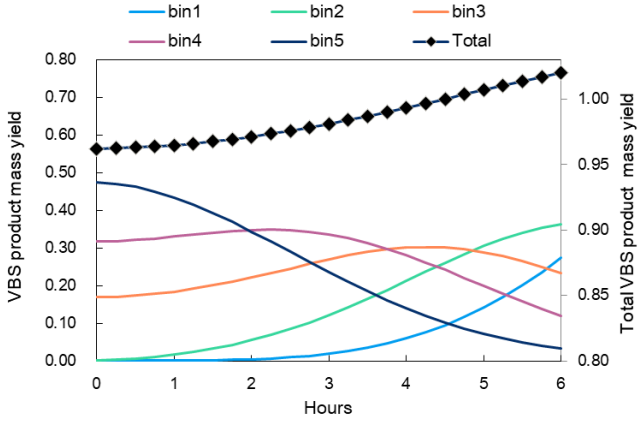

Figure 7 Aging an initial VBS product distribution that favors higher volatility bins (i.e., near bin 5) using the CAMx 1.5D VBS scheme with [OH] = 5 ×10^5 molecule/cm^3 and k_{OH} = 2 ×10^{-11} cm^3/molecule/s changes the volatility distribution to favor lower volatility bins (i.e., near bin 1) and increases total VBS product mass yield (due to oxidation) and would increase aerosol yield (not shown because depends on total OA as illustrated by Figure 8).

4 Conclusions

We applied two commonly used air quality models to simulate SOA concentration and contributions from VOC, IVOC and SVOC emissions over China for July and November 2018, with emphasis on comparing the models and their sensitivity to assumptions within the VBS schemes. Five OA components, including POA, SOA formed from biogenic VOC (BSOA), anthropogenic VOC (ASOA), IVOC-SOA, and SVOC-SOA, were resolved. The POA contribution to total OA is less than 10% in July and ranges from 10% – 40% in November (except for Northeast China), indicating the dominant role of SOA. Both models suggest that SOA contributions from SVOC emissions are negligible but IVOC represents an important SOA precursor, especially during November when IVOC becomes the leading SOA contributor for all selected regions except PRD (accounting for 26% to 30% in PRD and 45% to 63% in NCP). Although our modelling results are subject to uncertainties discussed below,

https://doi.org/10.5194/egusphere-2022-1502
Preprint. Discussion started: 23 January 2023

the consistently large contribution of IVOC emissions to total OA indicates that future control policies should aim at reducing IVOC emissions as well as traditional VOC emissions.

While both models show generally consistent results in terms of the spatial distributions and seasonal variations of the resolved OA components, differences were found with simulated ASOA and BSOA concentrations. CMAQ tends to estimate higher BSOA concentration, while CAMx generates more ASOA. As a result, CMAQ results suggest that BSOA concentration is always higher than ASOA in November, while CAMx emphasizes the importance of ASOA. With the help of a conceptual model, we demonstrate that the higher ASOA simulated by CAMx is attributable to the aging effect on ASOA implemented in CAMx. In the CAMx 1.5D VBS, SOA formed in higher volatility bins is assumed to undergo further gas-phase oxidation by OH into lower volatility bins. It is estimated that with 6 hours of aging at a representative wintertime OH concentration of 5×10^5 molecules/cm^3, SOA aging could enhance ASOA concentration by an order of magnitude, or more, depending on the total ambient OA concentration. The CMAQ VBS implements a different SOA aging scheme that represents particle-phase oligomerization and has smaller impacts on total OA, or no impact, than the CAMx 1.5D VBS aging scheme. A brief literature survey reveals that a diverse variety of VBS schemes (aging or no-aging) and/or parameters are being used in air quality models and could greatly affect model simulations of OA in ways that may be difficult to anticipate. Results from this study emphasize that improved availability of advanced monitoring data that resolve OA constituents would improve model evaluation and therefore model development.

Financial support. This study has been supported by the National Natural Science Foundation of China (Grant NOs. 42005112, 42075144, 41105102) and the Shanghai Sail Program (no. 19YF1415600).

Competing interests. The contact author has declared that none of the authors has any competing interests.

References

An, J., Huang, C., Huang, D., Qin, M., Liu, H., Yan, R., Qiao, L., Zhou, M., Li, Y., Zhu, S., Wang, Q., Wang, H., 2022. Sources of organic aerosols in eastern China: A modeling study with high-resolution intermediate-volatility and semi-volatile organic compound emissions. Atmos. Chem. Phys. Discuss. 2022, 1-44.

Appel, K.W., Bash, J.O., Fahey, K.M., Foley, K.M., Gilliam, R.C., Hogrefe, C., Hutzell, W.T., Kang, D., Mathur, R., Murphy, B.N., Napelenok, S.L., Nolte, C.G., Pleim, J.E., Pouliot, G.A., Pye, H.O.T., Ran, L., Roselle, S.J., Sarwar, G., Schwede, D.B., Sidi, F.I., Spero, T.L., Wong, D.C., 2021. The Community Multiscale Air Quality (CMAQ) model versions 5.3 and 5.3.1: system updates and evaluation. Geoscientific Model Development 14(5), 2867-2897.

Cao, J.J., Lee, S.C., Ho, K.F., Zou, S.C., Fung, K., Li, Y., Watson, J.G., Chow, J.C., 2004. Spatial and

https://doi.org/10.5194/egusphere-2022-1502
Preprint. Discussion started: 23 January 2023

seasonal variations of atmospheric organic carbon and elemental carbon in Pearl River Delta Region, China. Atmospheric Environment 38(27), 4447-4456.

Castro, L.M., Pio, C.A., Harrison, R.M., Smith, D.J.T., 1999. Carbonaceous aerosol in urban and rural European atmospheres: estimation of secondary organic carbon concentrations. Atmospheric Environment 33(17), 2771-2781.

Chang, X., Zhao, B., Zheng, H., Wang, S., Cai, S., Guo, F., Gui, P., Huang, G., Wu, D., Han, L., Xing, J., Man, H., Hu, R., Liang, C., Xu, Q., Qiu, X., Ding, D., Liu, K., Han, R., Robinson, A.L., Donahue, N.M., 2022. Article Full-volatility emission framework corrects missing and underestimated secondary organic aerosol sources. One Earth 5(4), 403-412.

Chen, X., Zhang, Y., Zhao, J., Liu, Y., Shen, C., Wu, L., Wang, X., Fan, Q., Zhou, S., Hang, J., 2021. Regional modeling of secondary organic aerosol formation over eastern China: The impact of uptake coefficients of dicarbonyls and semivolatile process of primary organic aerosol. Science of the Total Environment 793.

Cheng, Y.-l., Li, T.-t., Bai, Y.-h., Li, J.-l., Liu, Z.-r., Wang, X.-s., 2009. Numerical simulation study of SOA in Pearl River Delta region. Huan jing ke xue= Huanjing kexue 30(12), 3441-3447.

Donahue, N.M., Robinson, A.L., Stanier, C.O., Pandis, S.N., 2006. Coupled partitioning, dilution, and chemical aging of semivolatile organics. Environmental Science & Technology 40(8), 2635-2643.

Donahue, N.M., Robinson, A.L., Pandis, S.N., Kroll, J.H., Worsnop, D.L., 2009. Rethinking organic aerosols: Semivolatile emissions and photochemical aging. Geochimica Et Cosmochimica Acta 73(13), A299-A299.

Dunker, A.M., 2015. Path-integral method for the source apportionment of photochemical pollutants. *Geoscientific Model Development*, *8*(6), pp.1763-1773.

Dunker, A.M., Koo, B., Yarwood, G., 2019. Source apportionment of organic aerosol and ozone and the effects of emission reductions. Atmospheric Environment 198, 89-101.

Feng, Y., Chen, Y., Guo, H., Zhi, G., Xiong, S., Li, J., Sheng, G., Fu, J., 2009. Characteristics of organic and elemental carbon in PM2.5 samples in Shanghai, China. Atmospheric Research 92(4), 434-442.

Hayes, P. L., Carlton, A. G., Baker, K. R., Ahmadov, R., Washenfelder, R. A., Alvarez, S., ... & Jimenez, J. L. (2015). Modeling the formation and aging of secondary organic aerosols in Los Angeles during CalNex 2010. *Atmospheric Chemistry and Physics*, *15*(10), 5773-5801.

Hodzic, A., Kasibhatla, P.S., Jo, D.S., Cappa, C.D., Jimenez, J.L., Madronich, S., Park, R.J., 2016. Rethinking the global secondary organic aerosol (SOA) budget: stronger production, faster removal, shorter lifetime. Atmos. Chem. Phys. 16(12), 7917-7941.

Huang, L., Wang, Q., Wang, Y., Emery, C., Zhu, A., Zhu, Y., Yin, S., Yarwood, G., Zhang, K., Li, L., 2021. Simulation of secondary organic aerosol over the Yangtze River Delta region: The impacts from the emissions of intermediate volatility organic compounds and the SOA modeling framework. Atmospheric Environment 246.

Kampa, M., Castanas, E., 2008. Human health effects of air pollution. Environmental Pollution 151(2), 362-367.

Koo, B., Knipping, E., Yarwood, G., 2014. 1.5-Dimensional volatility basis set approach for modeling organic aerosol in CAMx and CMAQ. Atmospheric Environment 95, 158-164.

Li, J., Zhang, M., Tang, G., Sun, Y., Wu, F., Xu, Y., 2019. Assessment of dicarbonyl contributions to secondary organic aerosols over China using RAMS-CMAQ. Atmospheric Chemistry and

https://doi.org/10.5194/egusphere-2022-1502
Preprint. Discussion started: 23 January 2023

Physics 19(9), 6481-6495.

Li, L., Li, Q., Huang, L., Wang, Q., Zhu, A., Xu, J., Liu, Z., Li, H., Shi, L., Li, R., Azari, M., Wang, Y., Zhang, X., Liu, Z., Zhu, Y., Zhang, K., Xue, S., Ooi, M.C.G., Zhang, D., Chan, A., 2020. Air quality changes during the COVID-19 lockdown over the Yangtze River Delta Region: An insight into the impact of human activity pattern changes on air pollution variation. Science of the Total Environment 732.

Lin, J., An, J., Qu, Y., Chen, Y., Li, Y., Tang, Y., Wang, F., Xiang, W., 2016. Local and distant source contributions to secondary organic aerosol in the Beijing urban area in summer. Atmospheric Environment 124, 176-185.

Liu, H., Man, H., Cui, H., Wang, Y., Deng, F., Wang, Y., Yang, X., Xiao, Q., Zhang, Q., Ding, Y., He, K., 2017. An updated emission inventory of vehicular VOCs and IVOCs in China. Atmos. Chem. Phys. 17(20), 12709-12724.

Liu, J., Shen, J., Cheng, Z., Wang, P., Ying, Q., Zhao, Q., Zhang, Y., Zhao, Y., Fu, Q., 2020. Source apportionment and regional transport of anthropogenic secondary organic aerosol during winter pollution periods in the Yangtze River Delta, China. Science of the Total Environment 710.

Liu, Y.Z., Jia, R., Dai, T., Xie, Y.K., Shi, G.Y., 2014. A Review of Aerosol Optical Properties and Radiative Effects. Journal of Meteorological Research 28(6), 1003-1028.

Miao, R., Chen, Q., Shrivastava, M., Chen, Y., Zhang, L., Hu, J., Zheng, Y., Liao, K., 2021. Process-based and observation-constrained SOA simulations in China: the role of semivolatile and intermediate-volatility organic compounds and OH levels. Atmospheric Chemistry and Physics 21(21), 16183-16201.

Murphy, B.N., Woody, M.C., Jimenez, J.L., Carlton, A.M.G., Hayes, P.L., Liu, S., Ng, N.L., Russell, L.M., Setyan, A., Xu, L., Young, J., Zaveri, R.A., Zhang, Q., Pye, H.O.T., 2017. Semivolatile POA and parameterized total combustion SOA in CMAQv5.2: impacts on source strength and partitioning. Atmospheric Chemistry and Physics 17(18), 11107-11133.

Murphy, D.M., Cziczo, D.J., Froyd, K.D., Hudson, P.K., Matthew, B.M., Middlebrook, A.M., Peltier, R.E., Sullivan, A., Thomson, D.S., Weber, R.J., 2006. Single-particle mass spectrometry of tropospheric aerosol particles. Journal of Geophysical Research-Atmospheres 111(D23).

Nenes, A., Pandis, S.N., Pilinis, C., 1998. ISORROPIA: A new thermodynamic equilibrium model for multiphase multicomponent inorganic aerosols. Aquatic Geochemistry 4(1), 123-152.

Pankow, J.F., 1994. An absorption model of the gas/aerosol partitioning involved in the formation of secondary organic aerosol. Atmospheric environment (1994) 28(2), 189-193.

Pye, H.O.T., Ward-Caviness, C.K., Murphy, B.N., Appel, K.W., Seltzer, K.M., 2021. Secondary organic aerosol association with cardiorespiratory disease mortality in the United States. Nature Communications 12(1).

US EPA, 2019, *Overview of AERO7 and AERO7i*, https://github.com/USEPA/CMAQ/blob/5.3.2/DOCS/Release_Notes/aero7_overview.md

Ramboll, 2021. User's Guide: Comprehensive Air quality Model with extensions, Version 7.1. Available at: www.camx.com. Accessed on 25th September 2021

Robinson, A.L., Donahue, N.M., Shrivastava, M.K., Weitkamp, E.A., Sage, A.M., Grieshop, A.P., Lane, T.E., Pierce, J.R., Pandis, S.N., 2007. Rethinking organic aerosols: Semivolatile emissions and photochemical aging. Science 315(5816), 1259-1262.

Skamarock, W.C., Klemp, J.B., 2008. A time-split nonhydrostatic atmospheric model for weather

https://doi.org/10.5194/egusphere-2022-1502
Preprint. Discussion started: 23 January 2023

research and forecasting applications. Journal of Computational Physics 227(7), 3465-3485.

Wu, L., Ling, Z., Shao, M., Liu, H., Lu, S., Zhou, S., Guo, J., Mao, J., Hang, J., Wang, X., 2021. Roles of Semivolatile/Intermediate-Volatility Organic Compounds on SOA Formation Over China During a Pollution Episode: Sensitivity Analysis and Implications for Future Studies. Journal of Geophysical Research-Atmospheres 126(8).

Wu, L., Wang, X., Lu, S., Shao, M., Ling, Z., 2019. Emission inventory of semi-volatile and intermediate-volatility organic compounds and their effects on secondary organic aerosol over the Pearl River Delta region. Atmospheric Chemistry and Physics 19(12), 8141-8161.

Xie, Y.-B., Chen, J., Li, W., 2014. An assessment of PM2.5 related health risks and impaired values of Beijing residents in a consecutive high-level exposure during heavy haze days. Huan jing ke xue= Huanjing kexue 35(1), 1-8.

Yao, T., Li, Y., Gao, J., Fung, J.C.H., Wang, S., Li, Y., Chan, C.K., Lau, A.K.H., 2020. Source apportionment of secondary organic aerosols in the Pearl River Delta region: Contribution from the oxidation of semi-volatile and intermediate volatility primary organic aerosols. Atmospheric Environment 222.

Yarwood, G., Morris, R.E. and Wilson, G.M., 2007. Particulate matter source apportionment technology (PSAT) in the CAMx photochemical grid model. In Air pollution modeling and its application XVII (pp. 478-492). Springer, Boston, MA.

Yarwood, G., Jung, J., Whitten, G.Z., Heo, G., Mellberg, J., Estes, M., 2010. UPDATES TO THE CARBON BOND MECHANISM FOR VERSION 6 (CB6).

Zhang, L., Brook, J.R., Vet, R., 2003. A revised parameterization for gaseous dry deposition in air-quality models. Atmospheric Chemistry and Physics 3, 2067-2082.

Zhang, Q., Jimenez, J.L., Canagaratna, M.R., Allan, J.D., Coe, H., Ulbrich, I., Alfarra, M.R., Takami, A., Middlebrook, A.M., Sun, Y.L., Dzepina, K., Dunlea, E., Docherty, K., DeCarlo, P.F., Salcedo, D., Onasch, T., Jayne, J.T., Miyoshi, T., Shimono, A., Hatakeyama, S., Takegawa, N., Kondo, Y., Schneider, J., Drewnick, F., Borrmann, S., Weimer, S., Demerjian, K., Williams, P., Bower, K., Bahreini, R., Cottrell, L., Griffin, R.J., Rautiainen, J., Sun, J.Y., Zhang, Y.M., Worsnop, D.R., 2007. Ubiquity and dominance of oxygenated species in organic aerosols in anthropogenically-influenced Northern Hemisphere midlatitudes. Geophysical Research Letters 34(13).

Zhang, X., Cappa, C.D., Jathar, S.H., McVay, R.C., Ensberg, J.J., Kleeman, M.J., Seinfeld, J.H., 2014. Influence of vapor wall loss in laboratory chambers on yields of secondary organic aerosol. Proceedings of the National Academy of Sciences of the United States of America 111(16), 5802-5807.